The limits of the RICH technique

P. Glässel

Universität Heidelberg, 69120 Heidelberg, Germany

Abstract

The particle identification performance limits of the RICH technique are discussed both from a principal point of view and with regard to present state-of-the-art technology.

1 Introduction

The RICH (ring image Cherenkov) technique has evolved into a powerful experimental tool since the publication of the first, seminal paper [1]. The field is still vigorously developing due to new ideas and progress in technology of radiators, optics, and photon detectors. The purpose of this review is to explore the principal and practical limits of the RICH technique achievable with present state of the art technology, focusing on the main purpose of the RICH: particle identification. Many points touched upon are covered in much more detail in specialized papers in these proceedings.

2 Basic Cherenkov quantities and relations

The operation of Cherenkov counters is governed by the basic relation

$$\cos\theta = \frac{1}{n\beta} \tag{1}$$

which connects the emission angle θ of Cherenkov photons, the velocity β of the charged particle and the index of refraction n of the radiator medium. This leads to a velocity threshold, expressed by the Lorentz factor

$$\gamma_t = (1 - 1/n^2)^{-\frac{1}{2}} \tag{2}$$

The spectrum of Cherenkov photons is white with respect to photon energy and scales as $L \sin^2\theta$, giving a total of N detected photons for a radiator of length L:

$$N = N_0 L z^2 \sin^2\theta \tag{3}$$

(In the following, the charge of the passing particle z is assumed to be unity). The quantity given by eq. 3 is the mean or expected value, the distribution is Poissonian. For a photon detector with quantum efficiency Q, a total transmission T of radiator and window and a mirror reflectivity M (if present) the proportionality factor N_0, called the *figure of merit*, is

$$N_0 = \frac{\alpha}{\hbar c}\int Q\,T\,R\;\mathrm{d}E \tag{4}$$

For $\beta \to 1$ the Cherenkov angle approaches the *asymptotic* value θ_{max} related to threshold as

$$\sin^2\theta_{max} = \frac{1}{\gamma_{\mathrm{t}}^2} = \frac{1}{\eta_{\mathrm{t}}^2 + 1} \tag{5}$$

with an expected number of detected Cherenkov photons

$$N_{max} = \frac{N_0 L}{\gamma_{\mathrm{t}}^2} \tag{6}$$

For non-asymptotic cases, the mean number of detected Cherenkov photons is lower:

$$\frac{N}{N_{max}} = \frac{\gamma^2 - \gamma_{\mathrm{t}}^2}{\gamma^2 - 1} = \frac{\sin^2\theta}{\sin^2\theta_{max}} = 1 - \frac{\eta_{\mathrm{t}}^2}{\eta^2} \tag{7}$$

Here the quantity $\eta = \beta\gamma$ has been introduced, trivially related to the Lorentz factor as $\eta^2 = \gamma^2 - 1$. It directly relates to particle momentum ($p = \beta\gamma m$).

3 RICH observables

A RICH measures the *space* directions of N Cherenkov photons for a charged particle above threshold traversing the radiator, i.e. a set $\{\vec{u}_i\}$ of unity vectors. The sensitivity to direction only is not exact, due to spherical aberrations in the optics or finite radiator thickness in the case of proximity focusing, or due to detection outside the focal plane (approximation of curved focal surfaces by flat detectors), but typically it is quite good.

The set $\{\vec{u}_i\}$ defines a cone with the cone axis coinciding with the average direction of the charged particle $\vec{u}_p$. The photons subtend angles θ_i with respect to the cone axis. The best guess for the true Cherenkov angle is the mean

$$\theta_{\mathrm{c}} = \langle \theta_i \rangle \tag{8}$$

Whenever there are more photons detected than belong to one primary charged particle, we have a pattern recognition task that has to identify sets $\{\vec{u}_i\}$ that originate from one particle. This task requires a minimum number of detected photons per particle depending on

- the number of particles producing rings,
- whether the particle direction $\vec{u}_p$ is determined by external tracking elements or not,
- the number of background hits,
- the desired efficiency.

Background hits can be due to particles close to threshold that produce only very few photons, to photons from radiator scintillations, and to (Cherenkov) photons diffusely reflected on radiator walls from particles that cross the radiator at oblique angles, e.g. δ-rays.

Despite of the fact that these conditions vary a lot between different applications, there is a quite uniform consensus that a minimum of about 10 detected photons is required for adequate pattern recognition.

As an example, the CERES experiment has achieved 81 and 86% efficiency to find asymptotic electron rings in the high multiplicity environment of Pb-Au collisions at the CERN SPS [2].

4 Cherenkov angle and photons vs momentum

Cherenkov angle and number of detected photons depend in a universal way on the quantity η/η_{t}. In Fig. 1, both the number of photons normalized to the asymptotic value N_{max} (eq. 7) and the relative deviation of the Cherenkov angle from the asymptotic value

$$\frac{\sin\theta}{\sin\theta_{max}} = \sqrt{1 - \frac{\eta_{\mathrm{t}}^2}{\eta^2}} \tag{9}$$

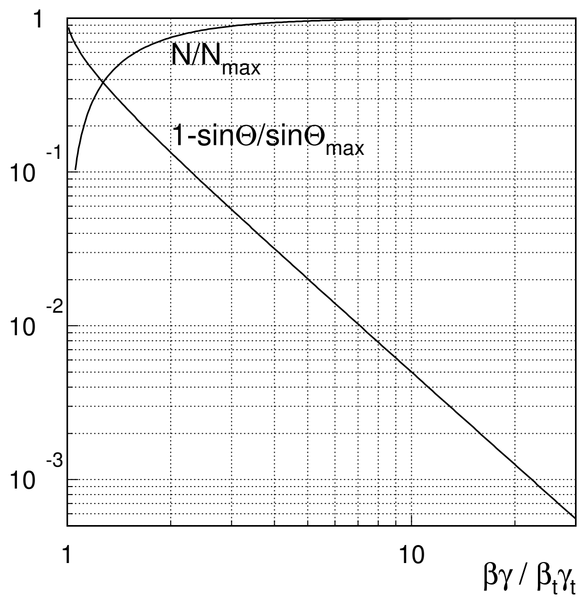

Fig. 1. Scaling plot for Cherenkov angle and number of photons

(also from eq. 7) are plotted against this scaling variable. The asymptotic Cherenkov angle is approached exponentially on a $\log \eta$-scale. (The sines of the angles make this an exact scaling relation even for large Cherenkov angles).

The range where momentum can be measured scales with mass, a feature the RICH shares with other particle identification techniques like TOF and $\mathrm{d}E/\mathrm{d}x$. The upper limit of η is determined by the resolution on the Cherenkov angle. For a desired resolution σ_η/η $(= \sigma_\mathrm{p}/p)$ one gets

$$\eta_{max} \approx \eta_\mathrm{t} \sqrt{\frac{\sigma_\eta}{\eta} \Big/ \frac{\sigma_{\theta_\mathrm{c}}}{\theta_{max}}} \tag{10}$$

The lower limit comes from pattern recognition and is due to the decrease in the number of detected photons towards threshold (eq. 3). For $\eta = \sqrt{2}\eta_\mathrm{t}$, e.g., we get $N = \frac{1}{2} N_{max}$ at a Cherenkov angle $\sin\theta = \sqrt{1/2}\,\sin\theta_{max}$.

5 Radiator length

The minimum radiator length giving enough detected photons is one of the most serious limitations of the RICH technique as detector size is one of the dominant cost factors for a system containing a RICH. This minimum length can be read from Fig. 2 for a range of N_0-values. The relation can be also read inversely: if the space available for the radiator is fixed by external constraints, the required N_0 can be read off. It has to be kept in mind that N is lower than N_{max} at the lower η-limit.

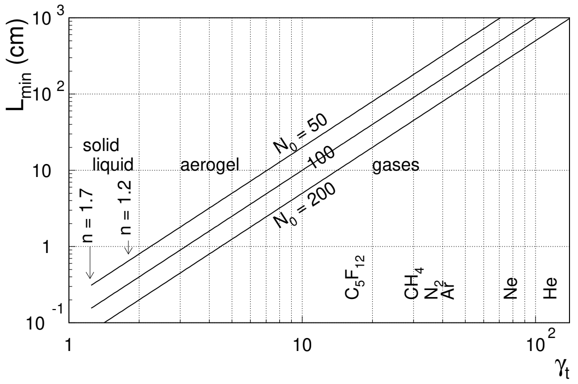

Fig. 2. Minimum radiator length vs γ_t for $N_{max} = 10$ and N_0 in the range 50 to 200.

In general, solid and liquid radiators require $L \leq 1$ cm. For the highest indices of refraction, tricks are needed to avoid trapping of the Cherenkov photons by internal reflection, e.g. by tilting the radiator, by giving it a sawtooth-shaped surface[3], or by the DIRC method [4]. Among liquid radiators, C_5F_{12} and C_6F_{14} are noteworthy because of their UV transparency [5].

Gas radiators are typically in the range $L \geq 1$ m, except for the densest gases like C_5F_{12} or for very high N_0-values.

Highly transparent qualities of aerogel, filling the gap between solid/liquid and gas, have recently been used for RICH radiators [6].

6 Optics schemes

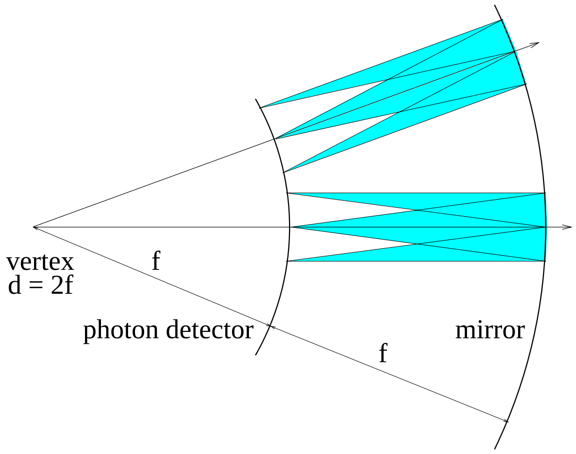

Fig. 3. Classical RICH geometry

The classical RICH arrangement is shown in Fig. 3. It allows large solid angles with one continuous – although maybe segmented – mirror. The focal surface, a sphere, usually has to be approximated by piece-wise flat detectors.

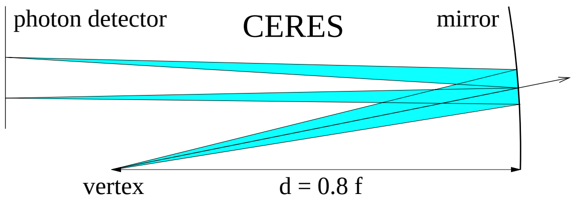

Fig. 4. CERES RICH geometry

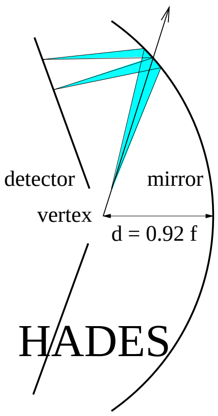

Fig. 5. HADES RICH geometry

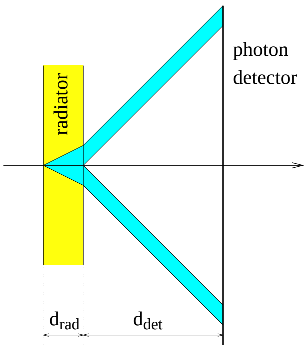

Fig. 6. Proximity focusing scheme

The position of the particle vertex, at the mirror center for the classical geometry, can be moved freely, however. Two examples are shown: the CERES and HADES setups, both with the vertex closer to the mirror than the photon detector. For the acceptance of CERES [2,7] to 15°, this has the advantage of a flat focal surface. HADES [8] goes to the other extreme of a very large solid angle from 15 to 85°, approximating the focal surface by a polygonal cone.

For solid and liquid radiators usually the 'proximity focusing' scheme is adopted, as shown in Fig. 6. Here a thin slab of radiator emits the Cherenkov photons which expand in a space between radiator and photon detector. The sharpness of the Cherenkov rings is determined by the ratio of radiator thickness and detector distance. Quite compact designs are possible.

Table 1
Figures of merit for a few detector/window combinations

photon detector	window	mirror	N_0	ref
TMAE / gas	quartz	yes	75	[7]
TMAE / gas	CaF_2^*	yes	135	[7]
reflective CsI / gas	CaF_2	yes	120	[8]
reflective CsI / gas	quartz	–	41	[10]
PM (visible)	glass	yes	47	[6]
PM (visible)	glass + PTP	yes	55	[12]
PM (170 nm)	quartz	yes	70–108	[13,14]

* cutoff from CH_4 radiator

7 Photon detectors

The state-of-the-art of RICH photon detectors is covered extensively in this conference. Here, only a summary is given.

Strong interest in the RICH technique started with the advent of gas photon detectors using gaseous photo-sensitive agents like TEA, TMAE etc. The next generation of RICH gas photon detectors relies mostly on solid photo-cathodes. CsI is the most developed material; its characteristics are similar to TMAE. Studies with visible light photo-cathodes for use in gas detectors look promising [9].

With the solid photo-cathodes, very compact gas detectors with signal integration times as low as 10 ns are possible. This allows to use them in high-rate and trigger applications.

Photo-multipliers, both conventional and multi-anode types are also widely used [4,6,11–14]. The HPD (hybrid photo diode) [15,16], a vacuum photo-cathode read out with an imaging electric field and a silicon pad detector, seems to become competitive for large sizes.

The overall performance, reflected by the figure of merit N_0 depends, of course, on the combination photo-cathode/detector/mirror/window/radiator. Proven figures of merit for a few combinations detector/window are given in Table 1. This table is not meant as an exhaustive list but rather intended to show the typical performances.

8 Contributions to Cherenkov angle resolution

As will be discussed in the next section, the particle identification performance is tied to Cherenkov angle resolution. There are a number of contributions to single photon resolution, of which some will be discussed in more detail:

(1) optics errors: mirror quality, spherical aberration, approximation of curved focal surfaces by flat detectors
(2) readout accuracy, depending on granularity and quality of interpolation,
(3) multiple scattering of the charged particle in the radiator,
(4) track bending due to magnetic (stray) fields,
(5) chromatic aberrations due to variation of the index of refraction over bandwidth.

These contributions are independent and add in quadrature.

The single photon contributions enter into the Cherenkov angle resolution:

$$\sigma_{\theta_c} = \frac{\sigma_\theta}{\sqrt{N}} \tag{11}$$

If the photon hits are used to determine the ring center, N under the square root is replaced by $N-1$. The ring center resolution, by the way, which is the tracking resolution of the RICH, is given by [17]

$$\sigma_{\theta_p} = \sqrt{\frac{2}{N-2}}\,\sigma_\theta \tag{12}$$

In the following, we will discuss the contributions of multiple scattering, magnetic fields, and chromatic aberrations in more detail. A more thorough discussion is given in [17].

8.1 Multiple scattering

The mean direction of the charged particle in the radiator deviates from the initial one – or from the one after the radiator – by $\sigma_{\theta_p} = \theta_0/\sqrt{2}$, where θ_0 is the well-known rms angular deflection due to multiple scattering after traversal of the radiator, projected in a plane [18]. The quantity σ_{θ_p} is relevant for the connection of a Cherenkov ring with an external particle track.

The direction of the charged particle *within the radiator* is also subject to multiple scattering, its rms deviation from the *mean* direction is

$$\sigma_{\theta_i} = \frac{\theta_0}{\sqrt{6}} \tag{13}$$

This term is the single photon resolution due to multiple scattering. It leads to a smearing of the Cherenkov ring. The resolution of the Cherenkov angle $\sigma_{\theta_c} = \sigma_{\langle\theta_i\rangle} = \sigma_{\theta_i}/\sqrt{N}$ based on N photons is independent of radiator length, since θ_0 scales as $\sqrt{L}$ in the same way as $\sqrt{N}$.

As we will see below, multiple scattering is negligible compared to chromatic aberrations for the typical radiator lengths quoted above. There are, however, RICH applications with much longer radiators with a dominating contribution from multiple scattering, like the proposed AQUA-RICH [16]. In this case, the observed σ_{θ_i} can be used to *measure* multiple scattering and infer the particle momentum. Such a scheme allows particle identification without external measurement of momentum.

8.2 Deflection in magnetic fields

Many experiment rely on tracking in magnetic field for momentum determination, so one has to worry about magnetic (stray) fields inside the RICH radiator. For the simple case of a homogeneous field component perpendicular to the charged particle trajectory, a total bending of

$$\Delta\theta = \frac{0.3(\mathrm{GeV/c\,m^{-1}\,T^{-1}})B_\perp L}{p} \tag{14}$$

occurs. The rms angular error is just $\sigma_{\theta_i} = \Delta\theta/\sqrt{12}$. This contribution has the same momentum scaling as the multiple scattering contribution; the scaling with radiator length L, however, is different: $\theta_{\mathrm{msc}} \propto \sqrt{L}$ vs $\theta_{mag} \propto L$.

Two examples are given in Table 2: 1 cm LiF and 1 m N_2. The last column gives the magnetic field value that leads to the same angular resolution as multiple scattering. For short solid or liquid radiators the tolerable fields are quite high; for gas radiators, the limits are much more stringent. As we will see in the next section, multiple scattering is usually small compared to chromatic aberrations, allowing larger fields than given in the table.

Table 2
Examples of multiple scattering and magnetic deflection

material	L	mult. scatt.	$B_\perp$
		σ_θ @ 1 GeV/c	for same σ_θ
LiF	1 cm	1.5 mrad	1.6 T
N_2	1 m	0.9 mrad	10 mT

8.3 Radiator chromatic dispersion

As shown in Fig. 7, in all radiator media the index of refraction increases towards higher photon energy [19]. The variation of the index of refraction over the observed bandwidth leads to a smearing of the Cherenkov angle. This is a very fundamental limitation that is hard to beat. As the effect increases with bandwidth at least linearly, this is also the price for improving N_0 via bandwidth. Achromatic optics exist, but only for RICH detectors with essentially zero solid angle. In all other cases, the only way to improve on the limit set by chromatic aberration is radiator length, i.e. exploiting the $\sqrt{N}$ denominator in eq. 11 by detecting more photons.

The rms error on the single photon is

$$\sigma_{\theta_i} = \frac{\sigma_n}{\beta n^2 \sin\theta} \tag{15}$$

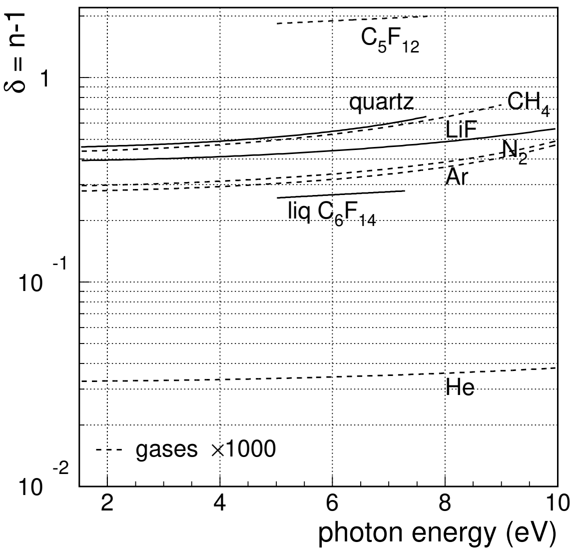

Fig. 7. Index of refraction -1 vs photon energy for some radiator media. Dashed lines are gases, scaled up $\times 1000$. Most of the data taken from parameterizations given in [17].

or, for $\beta \approx 1$ and $n \approx 1$

$$\frac{\sigma_{\theta_i}}{\theta_i} = \frac{1}{2} \cdot \frac{\sigma_n}{n-1} \tag{16}$$

were σ_n is the rms spread of the index of refraction over bandwidth weighted with QTR.

9 Angular resolution and particle identification

Particle identification with the RICH is based on distinguishing the Cherenkov angle for particles with known momentum. If one considers the quantity $\sin^2 \theta_c$, its difference for two masses m_1 and m_2 at momentum p is

$$\Delta \sin^2 \theta_c = \frac{m_2^2 - m_1^2}{n^2 p^2} = \frac{\Delta m^2}{n^2 p^2} \tag{17}$$

The quality of the separation is described by the number of standard deviations in this quantity, it can be calculated to be

$$n_\sigma = \frac{\beta^2 \Delta m^2}{2p^2} \Big/ \frac{\sigma_\beta}{\beta} = \frac{\beta^2 \Delta m^2}{2p^2 \tan \theta_c \sigma_{\theta_c}} \tag{18}$$

leading to an upper momentum limit for n_σ standard deviation separation of

$$p_{max} = \left(\frac{\beta^2 \Delta m^2 \eta_t}{2 n_\sigma \, \sigma_{\theta_c}} \right)^{\frac{1}{2}} \tag{19}$$

This upper limit is usually above the limit given by eq. 5 for the smaller of the two masses, meaning that the ring cannot be discriminated from an asymptotic one.

The lower momentum limit is due to the decreasing N/N_{max} and around

$$p_{min} \approx 1.4 \, \eta_t \, m \tag{20}$$

Table 3 gives chromatic errors for a range of radiators covering γ_t from 1.35 to 120. A number $N = 10$ detected photons are assumed to convert from single photon resolution to Cherenkov angle resolution. The bandwidth used assumes CsI photo cathodes for the solid and liquid, and TMAE operation for the gas radiators. The rms variation of the index of refraction is taken as

$\Delta n/\sqrt{18}$, i.e. a skewed triangular response, reflecting the near-linear rise of quantum efficiency with photon energy. (This is somewhat pessimistic since the upper cutoff is often also smooth due to window and mirror).

The main conclusions from Table 3 are:

- The chromatic errors exceed the multiple scattering contribution by large factors.
- The momentum range, expressed as the ratio p_{max}/p_{min} is limited to about 4 to 6. Larger ranges require two different radiators.
- There is a momentum range gap between liquids and gases, the reason why aerogel is attractive despite its problems [6].

Table 3
Examples for chromatic aberration limits

radiator	LiF	C_6F_{14}	C_5F_{12}	N_2	He
L	1 cm	1 cm	0.5 m	2 m	10 m
γ_t	1.35	1.62	16	41	120
bandwidth (eV)	6 - 7.7	6 - 7.3	5.5 - 7.7	5.5 - 7.7	5.5 - 10
$\sigma_n = \Delta n/\sqrt{18}$	0.009	0.0028	$30 \cdot 10^{-6}$	$12 \cdot 10^{-6}$	$5 \cdot 10^{-6}$
σ_{θ_i} (mrad)	5.4	2.8	0.45	0.40	0.13
σ_{θ_c} (mrad)	1.8	0.9	0.14	0.13	0.042
chromatic/msc	5	5	10	30	60
3σ separ. Kπ					
p_{max} (GeV/c)	4	7	50	100	330
p_{min} (GeV/c)	0.6	0.88	11	28	83

10 Summary

It has been shown that the principal limitations of the RICH for particle identification originate from the chromatic dispersion of radiators. The more practical limitations come from the figure of merit N_0 which dictates number of detectable photons *vs* system size. Of the factors governing N_0, a high value of the product QTR is more valuable than high bandwidth since the latter is payed for by chromatic aberrations. Improvements in the future will thus come from higher quantum efficiency photon converters.

References

[1] J. Seguinot and T. Ypsilantis, Nucl. Instr. and Meth. 142 (1977) 377

[2] E. Sokol, these proceedings F.8

[3] R. Mountain, these proceedings B.4

[4] B. Ratcliff, these proceedings C.3

[5] W. Adam et al., Nucl. Instr. and Meth. A 371 (1996) 12

[6] D. Ryckbosch, these proceedings C.1

[7] R. Baur et al., Nucl. Instr. and Meth. A 343 (1994) 87

[8] K. Zeitelhack et al., these proceedings D.3

[9] E. Shefer et al., these proceedings I.7

[10] F. Piuz, these proceedings D.1

[11] S. Korpar, these proceedings C.4

[12] V. Molchanov, these proceedings C.9

[13] J. Engelfried, these proceedings C.6

[14] T. Hemmick, these proceedings C.5

[15] J. Seguinot, these proceedings A.1

[16] T. Ypsilantis, these proceedings C.2

[17] T. Ypsilantis and J. Seguinot, Nucl. Instr. and Meth. A 343 (1994) 30

[18] C. Caso et al., Eur. Phys. J. C3 (1998) 1

[19] E.R. Hayes, R.A. Schluter, A. Tamosaitis, "Index and dispersion for some Cherenkov counter gases", ANL-6916 (1964)